The Journal of Engineering Geology
pISSN : 1226-5268 eISSN : 2287-7169
Vol. 33, No. 1, March, 2023, pp. 121-136
https://doi.org/10.9720/kseg.2023.1.121

RESEARCH ARTICLE

Microstructural Features and K-Ar Ages of Fault Gouges from Quaternary Faults along the Northern Yangsan Fault, SE Korea

Chang Oh Choo[1] · Tae Woo Chang[2] · Kounghoon Nam[3] · Jong-Tae Kim[4] · Chang-Ju Lee[5] · Gyo-Cheol Jeong[6*]

[1]Professor, Department of Earthquake Prevention Engineering, Andong National University
[2]Emeritus Professor, Department of Geology, Kyungpook National University
[3]Post-Doctor, College of Civil Engineering, Tongji University, China
[4]CEO and Principal Researcher, Nature and Tech Inc.
[5]CEO and Principal Researcher, Daeyeong Construction and Engineering
[6]Professor, Department of Earth and Environmental Sciences, Andong National University

Abstract

Microstructural characterization, identification of mineral assemblages, and K-Ar age dating of fault gouges from five Quaternary fault sites segmented along the northern Yangsan Fault, SE Korea were performed to understand formation condition and multiple activity of faults. The mean and median sizes of particles of bulk gouges vary among the studied faults: 1.75 μm and 1.43 μm for the Danguri Fault, 1.94 μm and 1.79 μm for the Yukjae Fault, 5.57 μm and 4.16 μm for the Yugye Fault, and 5.55 μm and 2.31 μm for the Bogyeongsa Fault. Fault gouges contain abundant secondary minerals, including smectite, chlorite, illite, kaolinite, laumontite, and mordenite, which are found in association with quartz and feldspar. K-Ar dating of the fault gouges (both bulk samples and separate size fractions) yields ages ranging from 59.1 to 18.8 Ma, with bulk ages of 47.6 Ma for the Yukjae Fault, 59.1 Ma for the Ansim Fault, 39.4 Ma for the Yugye Fault, and 22.6 Ma for the Bogyeongsa Fault. The finer fractions generally have younger K-Ar ages compared with the coarser fractions, and the finest fraction (<0.2 μm) is the youngest for each fault. Hydrothermal alteration of the gouges is considered to have occurred under low-temperature (100~200°C) conditions during faulting. Microstructural features and clay mineral assemblages of fault gouges and brecciated rocks should be considered when interpreting fault events and reactivation, in addition to age dating of faulting.

Keywords: fault rocks, K-Ar age dating, Yangsan Fault, fault gouge, clay minerals

OPEN ACCESS

***Corresponding author:** Gyo-Cheol Jeong
E-mail: jeong@anu.ac.kr

Received: 13 March, 2023
Revised: 27 March, 2023
Accepted: 28 March, 2023

Introduction

A series of seismic events, including 2016 Gyeongju earthquake and 2017 Pohang earthquake, on or near the Yangsan Fault in SE Korea have stimulated renewed interest in fault-related research in the country, which includes the study of fault activity, deep underground disposal, rock stability, and fault rock properties (Choo et al., 2020). The Yangsan Fault System (YSF), which is the largest and most active Quaternary fault on the Korean Peninsula, is of considerable interest both geologically and from the perspective of hazard mitigation. Based on the fault segmentation, paleoseimological data, and displacement of faults, maximum earthquakes of magnitude 7.3 were proposed for

the Yangsan Fault (Lee and Kyung, 2022). Movement on the YSF has been right-lateral strike-slip caused by NE-SW compression since the Eocene, including its most active period in the Late Miocene (Chang and Chang, 1998; Chang, 2001). The YFS shows evidence of multiple deformation events through geologic time. Until recent, more than 70 Quaternary faults have been identified at the southeastern part of the Korean Peninsula (Lee and Kyung, 2022). Some Quaternary faults have been found on the northern part of the Yangsan Fault as well as on the southern part, indicating that they resulted from segmentation by reactivation of preexisting faults.

Gouge zones in fault zones may record long movement histories of faults and information on faulting. Fault gouges form by interaction of very fine-grained materials through the pulverization of host rocks in fault-core zones and contains abundant clay minerals. Fault gouges commonly include a significant amount of various clay minerals formed by faulting, and the types of neoformed clay in gouge appear to be the results from wall-rock alteration in crushed materials and fluid chemistry, and temperatures at relatively low temperatures (Vrolijk and van der Pluijm, 1999; Solum et al., 2006; Haines and van der Pluijm, 2012).

K-Ar data for clay minerals have proved useful for constraining the age and evolution of faults, as well as in understanding the diagenetic change from smectite to illite and illite-smectite (I-S) interstratification (Velde and Renac, 1996; Vrolijk and van der Pluijm, 1999; Meunier et al., 2004). In particular, illite age analysis (IAA) can be used to estimate the age of authigenic illite formation (Pevear, 1992, 1999). Since the first reported K-Ar ages of clay gouges from the Dongrae Fault (Chang and Choo, 1998) and from the Yangsan Fault (Chang and Choo, 1999), more K-Ar ages of fault materials from the YFS have become available, together with ages obtained using other dating methods, including optically stimulated luminescence (OSL), electron spin resonance (ESR), and C- isotope dating (Chang, 2001 and references therein; Lee et al., 2015; Song et al., 2019, 2020; Lee and Kyung, 2022 and references therein).

Microstructural properties of fault gouges and fractured fault rocks, neoformed-mineral assemblages, particle size, and K-Ar age dating of fault gouges provide essential information that serves as a basis for understanding fault activity. For example, the mineral composition of a fault gouge affects the slip and friction coefficients of a fault and thereby has a strong influence on the frictional strength of a fault (Collettini et al., 2009; Tembe et al., 2010; Sakuma et al., 2022). In this study, microstructural characterization of fault rocks, identification of mineral assemblages, and K-Ar age dating on some Quaternary fault sites segmented along the northern Yangsan Fault, SE Korea were performed to better understand formation condition and multiple activity of the faults.

Geological Description of Fault Sites and Analytical Methods

In this study, Quaternary faults along the northern part of the Yangsan Fault, SE Korea were investigated. Faults were indentified in the Danguri, Yukjae, Ansim dam, Yugyeri, and Bogyongsa areas. It is noteworthy that all of the studied faults show a dextral sense of movement. The Danguri Fault is located north of the Byeokgye Fault in Gangdong-myeon, NW Gyeongju, SE Korea. Cretaceous granite and subvolcanic rocks were intruded into Cretaceous sedimentary rocks in the fault area. The Danguri Fault with N12°E / 83°NE developed along a valley, where the host sedimentary rocks in the northeast are in contact with Quaternary fluvial deposit (Fig. 1a). There are several fault gouge zones and striation,

which indicates a reverse strike-slip.

The Yukjae Fault is exposed at a road cutting in Sangdaeri, Cheongha-myeon, NW Pohang (Fig. 1b). The fault plane is oriented N78°W/40°NE, showing a dextral strike-slip sense of movement. The fault gouge, which consists of fine-grained clays, is composed of a dark blue layer and a greenish brown layer, each measuring 2~3 cm in thickness. Breccia zones are located on the both sides of the fault gouge. The host rocks of the fault consists of dark grey Cretaceous mudstone and dark grey sandstone. Clays in the matrix do not have a shape preferred orientation, although some residual fragments occur as crush trails generated by gradual shearing that define a foliation. These textures indicate a dextral sense of movement.

The Ansim Fault is exposed along a road cutting near the Ansim dam. The blackish grey fault gouge is a few cm wide and contains subangular or subrounded fragments of 0.5~1.5 cm in size. Clay particles are commonly aligned to define a foliation. In the damaged zone, greyish conglomerate and dark grey shale are in contact with the fault core zone. The matrix consists mostly of clays and traces of scattered pyrite, microcrystalline quartz, and feldspar. Altered large fragments contain networks of calcite veins.

The Quaternary Yugye Fault at Yugye dam is a reverse fault and extends along the contact between highly fractured volcanic rocks and Quaternary fluvial deposits. The fault developed along a valley and stream where the Yugye dam was constructed. In this study (Fig. 1c and 1d), the fault outcrop was investigated in 2002 before dam construction was completed. The fault core, which has a thickness of 2 m, is situated between damaged zones comprising alternating layers of Cretaceous dark green sandstone and reddish shale. The orientation of fault planes is N45°E/85°SE, and slip striation on the fault plane indicates a dextral sense of movement. Slickenside and slicken fibers of calcite are commonly found on vertical planes (Fig. 1d). The Yugye Fault is a reverse fault that separates Quaternary fan-type fluvial gravel from Cretaceous sedimentary rocks. Eastward-plunging striations and stretching of gravel beds parallel to the fault plane indicate reverse slip. This Quaternary reverse fault is intersected by a Quaternary strike-slip fault. Petrographic thin-section observation reveals at least four distinct episodes of fault movements.

The Bogyeongsa Fault is located along or near Bogyeongsa temple valley, NW Pohang. Dark purplish gouge and bluish grey gouge are identified at the bottom of a stream. The fault zone separates Cretaceous dacitic lapilli tuff from reddish sedimentary rocks (Fig. 1e and 1f), and the fault gouge zone has a width of 20~30 cm. The boundary between the fault gouge and the breccia zone is a fault plane oriented N15°E /70°NW and the slip indicates a dextral sense of movement. Clay foliation in the fault gouge defines a foliation, mainly comprising rounded residual fragments (Fig. 1g). Calcite veins indicate at least three faulting events. Domino-type fractures and ductile shearing in calcite veins are observed, indicating a dextral sense of movement (Fig. 1h and 1i). NE- or NNE-striking subsidiary strike-slip faults and shear fractures display a dextral sense of movement. The damage zone is characterized by a high density of fractures and veins, as well as associated subsidiary faults that formed during multiple faulting events.

Fault gouges were collected from the five studied faults. Clay-size minerals were separated from of the fault gouges by applying ultrasonic disaggregation, gravity settling, and high-speed centrifugation method. The bulk and clay fraction compositions of the gouge samples were determined by X-ray diffraction (XRD) analysis using a Philips X' Pert-PRO/MRD diffractometer with Ni-filtered CuK α radiation in the range of 3~65 °2 θ and 0.02° step for 3 s.

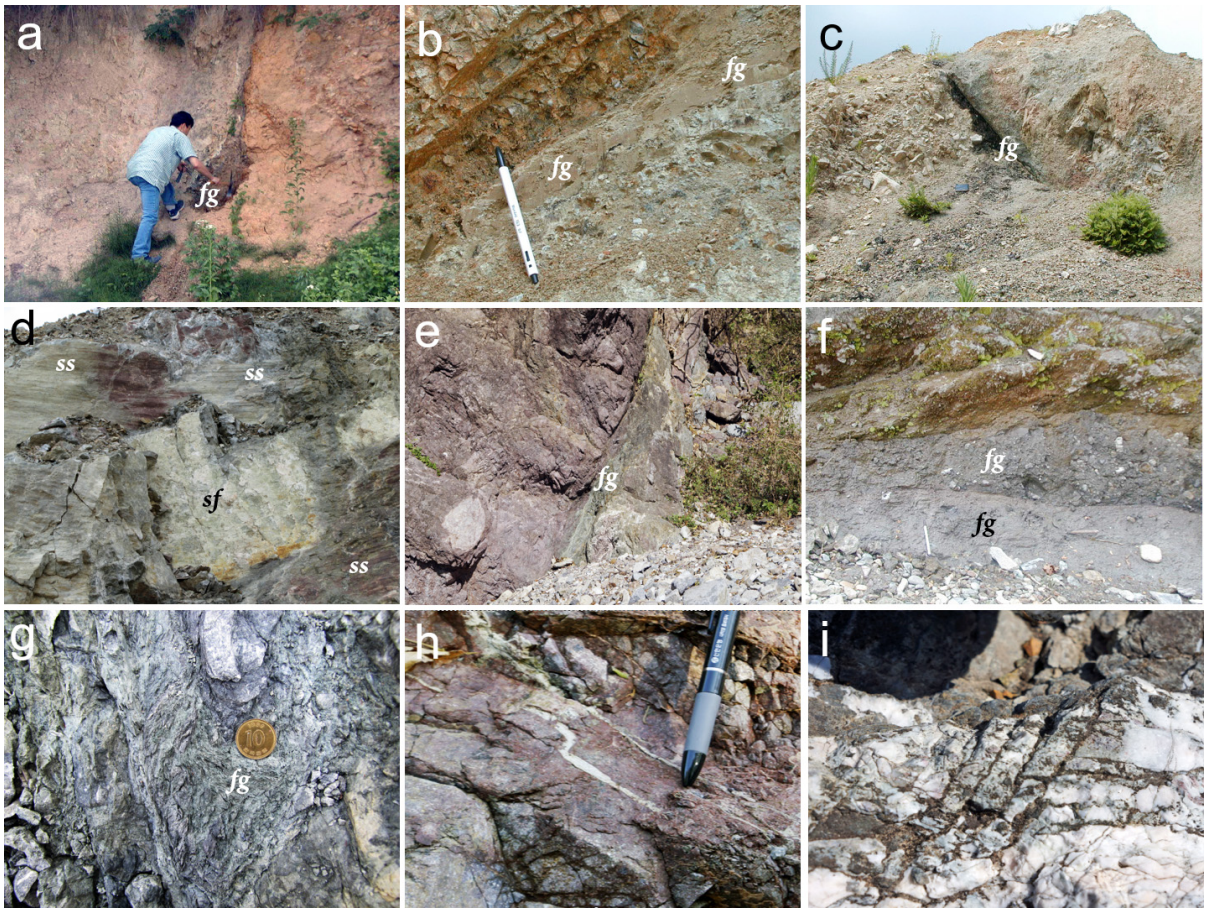

Fig. 1. Fault outcrops of the Yangsan Fault. (a) Danguri fault along the contact between basement rocks and Quatenary deposit, (b) Yukjae fault, (c) Yugyeri fault along the contact between volcanic rocks and Quaternary deposits with reverse faulting, (d) Yugyeri fault with slicken fibers, (e), (f) Bogyeongsa fault gouge, (g) Clay foliation surrounding residual fragments in Bogyeongsa fault gouge, (h) Calcite vein showing a dextral sense in Bogyeongsa fault, (i) Domino-type asymmetric boudins in calcite from Bogyeongsa fault indicating a dextral sense. fg: fault gouge, sf: slicken fiber, ss: slickenside.

Original particle-size distributions of bulk fault gouges were measured using a wet method and a laser diffraction particle-size analyzer (Malvern Mastersizer 2000) through the size range of 0.02~2,000 μm. The fault gouge samples were disaggregated by ultransonic agitation, following which the clay size fraction was obtained by centrifugation and gravitational sedimentation. Finally five particle-size fractions were separated: <0.2, 0.2~1.0, 1.0~2.0, 2.0, and >2.0 μm. Oriented clay-mineral aggregates from each size fraction were prepared on glass slides to characterize clay species in detail in the 3~40° 2 θ range. After obtaining reflection data from powdered samples, we performed quantitative analysis on constituent minerals in the gouge and fault rock samples based on Rietveld method using diffraction patterns. The polytype ratio of illite was calculated by comparing reflections at 2.58 Å and 2.80 Å (Tettenhorst and Corbató, 1993).

Microtextural observations and semi-quantitative chemical analyses were performed on untreated fresh portions of fault gouge and core samples using scanning electron microscopy (SEM) (JEOL JSM 840A and FE-SEM Hitachi S4200). A transmission electron microscope (TEM) (JEOL JEM-2010) with an accelerating voltage of 200 kV at Andong National University was used to observe nanometer-to micrometer-sized crystals. Samples of 2 g for each

particle-size fraction containing illite were used for K-Ar age dating at Geochron Laboratories Krueger Enterprises, Chelmsford, USA.

Results

Particle Size Distribution of Fault Gouges

Particle sizes of bulk gouges collected from the studied faults were measured, as shown in Table 1 and Fig. 2. The mean size and median size (d0.5) of particles of bulk gouges differ among the faults: 1.75 μm and 1.43 μm for Danguri, 1.94 μm and 1.79 μm for Yukjae, 5.57 μm and 4.16 μm for Yugye, and 5.55 μm and 2.31 μm for Bogyeongsa Faults, respectively. Average and finer particles are in the following order: Yugyeri > Boyeongsa > Yukjae > Danguri. Finer particles represented by d(0.1) and coarser particle by d(0.9) in samples from the Danguri and Yukjae faults are finer compared with those from the Yugye and Bogyeongsa faults.

Table 1. Particle-size distribution and surface area of bulk fault gouges

	Danguri	Yukjae	Yugye	Bogyeongsa
d(0.1) (μm)	0.53	0.83	1.54	0.62
d(0.5) (μm)	1.43	1.79	4.16	2.31
d(0.9) (μm)	3.43	3.22	11.57	14.63
Vol. weighted mean D (μm)	1.75	1.94	5.576	5.55
Specific surface area (m^2/g)	5.486	4.081	1.941	3.94

d(0.5) is the median size (at the 50th percentile) and d(0.1) and d(0.9) are the particle sizes at the 10th and 90th percentiles in the distribution.

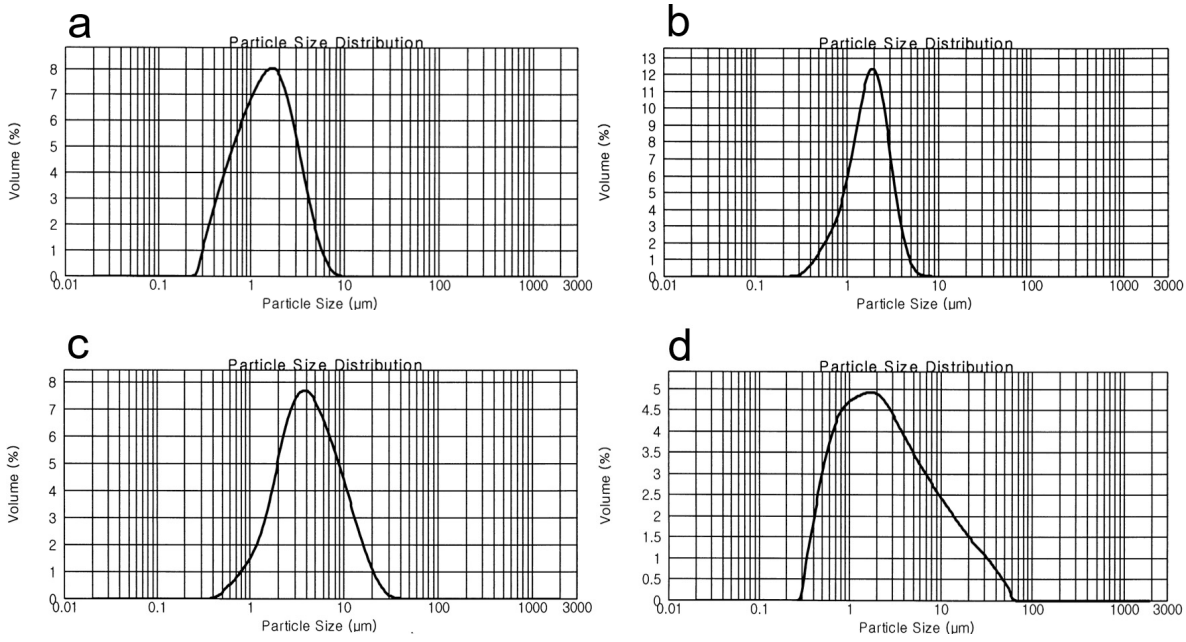

Fig. 2. Particle-size distribution of bulk fault gouge measured by laser particle analysis. (a) Danguri, (b) Yukjae, (c) Yugyeri, (d) Bogyeongsa.

Mineralogical Compositions of Fault Gouges

Mineral compositions of fault gouges calculated by XRD results are summarized in Table 2. Fault gouges contain abundant secondary minerals, including smectite, chlorite, illite, kaolinite, laumontite, and mordenite, which are found in association with quartz and feldspars. Mixed-layer minerals such as I/S, corrensite, or I/V are inferred to be absent, given the lack of phases at 3~5° 2θ. In the Danguri Fault, chlorite and illite are the main clay minerals, and calcite occurs as a secondary mineral. In gouge from the Yukjae Fault, chlorite is the most abundant clay mineral, followed by kaolinite and laumontite as clay minerals or alteration minerals. Of note, kaolinite occurs in the fault core center of the Yukjae Fault.

Table 2. Mineralogical compositions of fault gouges and fault-core rocks from the studied faults of the northern Yangsan Fault, as determined by XRD analysis (unit: wt.%)

Fault samples	Ch	Il	Ka	Sm	Lm	Md	Qz	Ab	Or	Hb	Cc
Danguri	26.1	26.5					5.4	29.5			12.6
Yukjae core center	23.3		13.6	2.9			9.6	50.7			
Yukjae core 10 cm	20.2				10.6		40.8	28.4			
Yukjae core 25 cm	24.0			2.2	10.8	9.0	22.4	31.7			
Ansim	16.8				7.1		30.5	22.8	22.8		
Yugye			17.1				17.4	23.0		36.5	6.0
Bogyeongsa-1	17.2	34.0					36.1	8.7			4.0
Bogyeongsa-2		26.7	6.8				51.8	6.4			8.3
Bogyeongsa-3	18.4	33.8					42.8				4.9
Bogyeongsa-4	14.4	14.6					21.5	4.1			45.4
Bogyeongsa-33	15.9	32.4					35.6		12.1		4.0
Bogyeongsa grey	17.8				9.0		1.7	22.6		33.1	15.8
Bogyeongsa reddish	18.5				7.7		19.5	54.4			

Ab: albite, Cc: calcite, Ch: chlorite, Hb: hornblende, Il: illite, Ka: kaolinite, Lm: laumontite, Md: mordenite, Or: orthoclase, Qz: quartz, Sm: smectite.

In addition, mordenite is present as a unique zeolite mineral in fault rocks located 25 cm from the inner gouge of the fault. This is the only species of zeolite found in faults along the northern Yangsan Fault. Calcite is observed in gouges from the Danguri, Yugye, and Bogyeongsa faults. In oriented samples, the presence of smectite, chlorite, illite, and kaolinite is clearly identified (Fig. 3).

The amounts of quartz and chlorite increase with increasing particle size in gouge from the Ansim and Bogyeongsa faults. The $1M_d$ type illite polytype is the main polytype in the fault gouges, but the $2M_1$ polytype also occurs in the Yukjae Fault gouge. Smectite and chlorite are the most abundant clay minerals in the studied fault gouges, with smectite being the dioctahedral species, as interpreted from the (060) reflection at 62.22~61.67 2θ (CuKα), which averages around 1.5 Å.

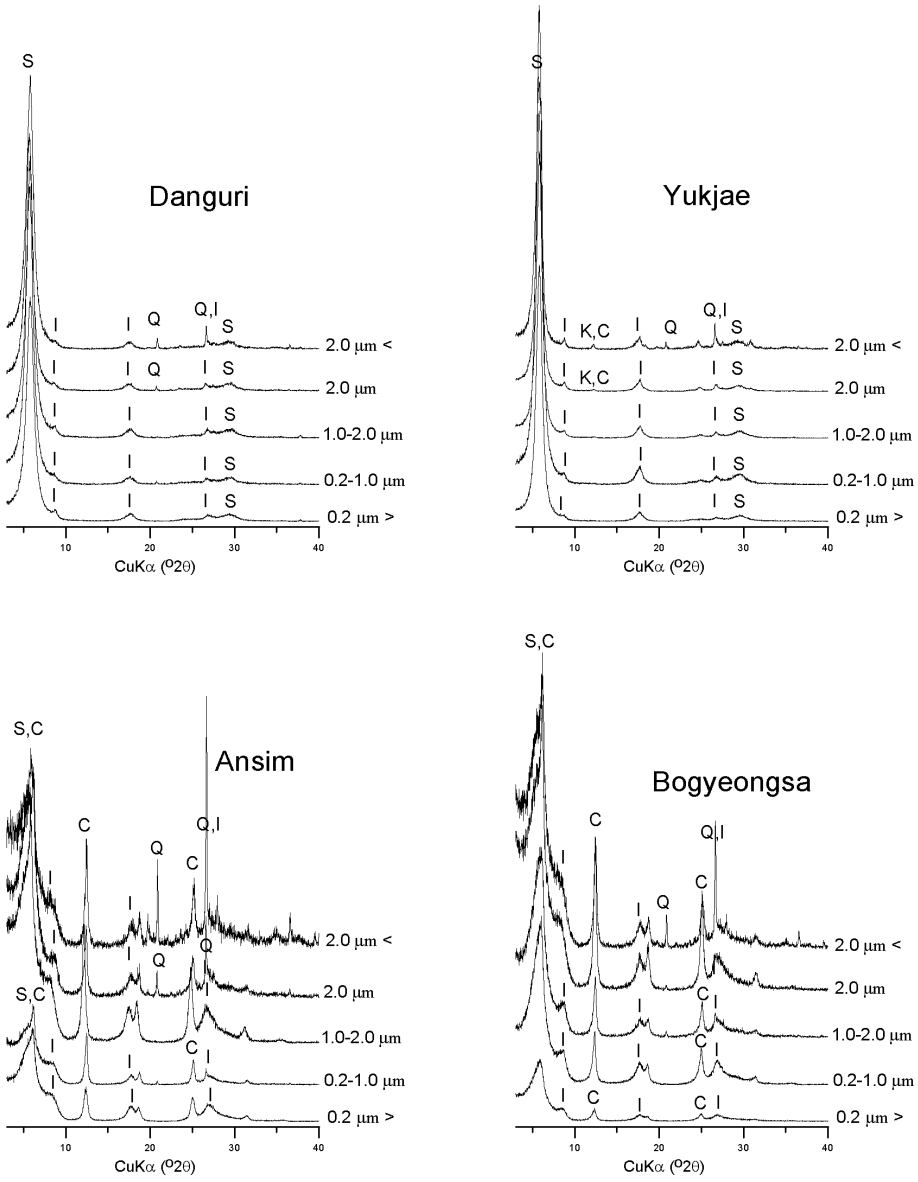

Fig. 3. X-ray powder diffraction patterns of oriented samples according to grain-size fraction. C: chliorite, K: kaolinite, I: illite, QL quartz, S: smectite.

Microstructural Properties of Fault Gouges

SEM and TEM observations show that the bulk fault gouges and fault rocks contain authigenic minerals and host minerals (Figs. 4~6). Establishment of the microstructural properties of fault gouges and fractured rocks can help to constrain the formation of secondary minerals and fracturing during faulting activity. For example, illite formed authigenically during faulting of the Danguri Fault (Fig. 4a). The illite flakes, which indicate poor crystallization, surround microcrystallites of quartz (~5 μm). Hematite crystals, which have been abraded to form rounded grains (Fig. 4b), contain 90.3 wt.% Fe_2O_3, 3.32 wt.% ZrO_2, 2.29 wt.% SiO_2, and 4.10 wt.% other elements (as oxides), indicating hematite with trace zircon.

Smectite flakes in the Yugye Fault gouge are poorly crystallized and have a honeycomb-like texture (Fig. 4c). Fractured minerals such as quartz and plagioclase are found in the damage zone of the Yugye Fault (Fig. 4d). A foliation defined by smectite and chlorite is well developed in the Bogyeongsa Fault gouge (Fig. 4e and 4f). Rounded residual grains are surrounded by a foliation defined by clay particles. The presence of a clay-defined foliation in fault gouge is generally regarded as evidence that faulting activity continued for a long period after the clay minerals formed, as the clay minerals formed immediately after a faulting event, and developed a shape preferred orientation in response to fault stresses during subsequent faulting events. Rotational abrasion of residual grains caused a reduction in grain size, and the clay matrix surrounding the grains served as a buffer to inhibit further size reduction, even if faulting-related stresses continued to be generated.

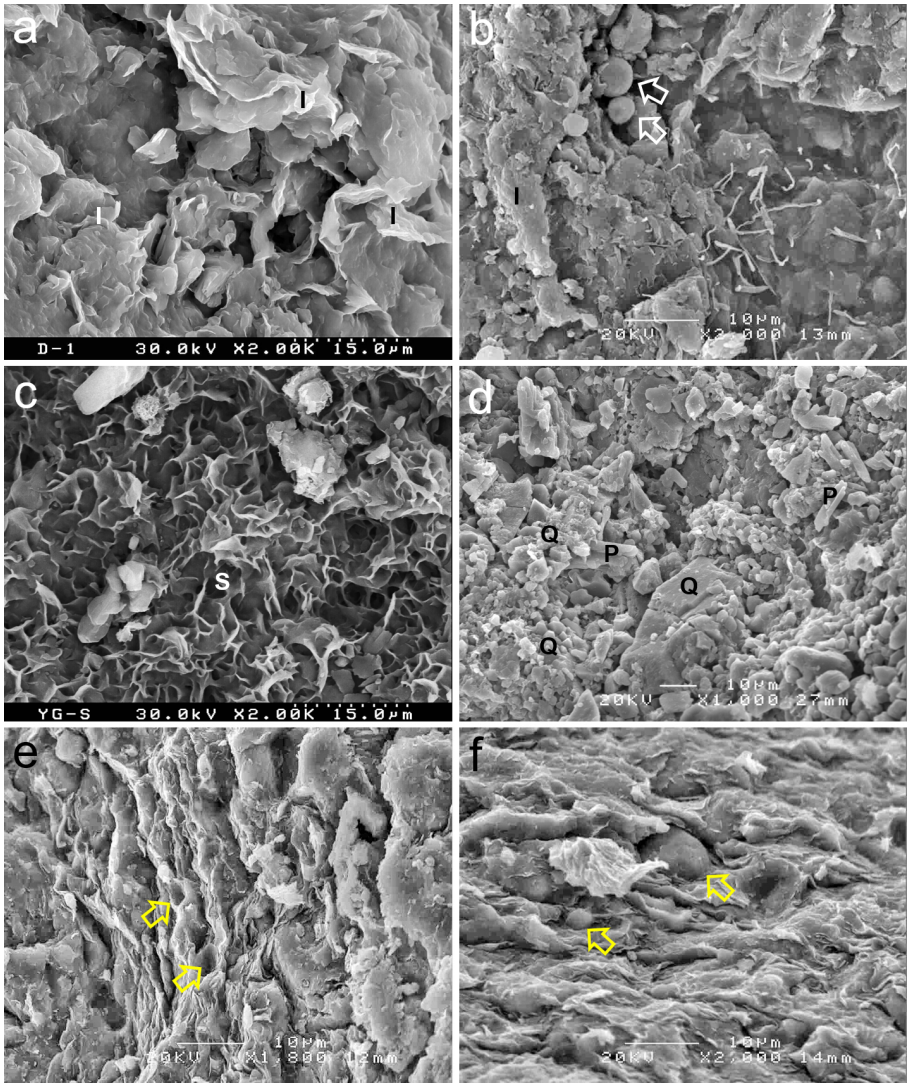

Fig. 4. SEM images of fault rocks. (a) Illite flakes from the Danguri Fault, (b) Rounded residual grains of iron oxides (arrowed) from the Danguri Fault, (c) Illite flakes from the Yugye Fault, (d) Fractured minerals, including quartz and plagioclase, from the damaged zone of the Yugye Fault, (e) Smectite and chlorite-defined foliation from the Bogyeongsa Fault. Note the vacant cavities (arrowed) of residual grains in the foliation after detachment. (f) Rounded residual grains (arrowed) in foliated gouge from the Bogyeongsa Fault. I: illite, Q: quartz, P: plagioclase, S: smectite.

In the Yukjae Fault samples, a clay-defined foliation composed of smectite is identified in the center of the fault core (Fig. 5a and 5b). The foliation is similar to that in other faults zone. Residual grains with sizes of <5 μm have survived as porphyritic fragments and are included in the clay-defined foliation. Fractured fault rocks, which occur 10 cm from the gouge center, contain laumontite and chlorite as secondary minerals (Fig. 5c~5e). Chlorite and laumontite are also common in fractured fault rocks near the gouge zone. Chlorite appears to have formed through direct precipitation rather than by replacement of original mafic minerals in the host rocks, as inferred from its occurrence as dense well-crystallized aggregates that resemble a honeycomb and lack any alteration textures inherited from other minerals.

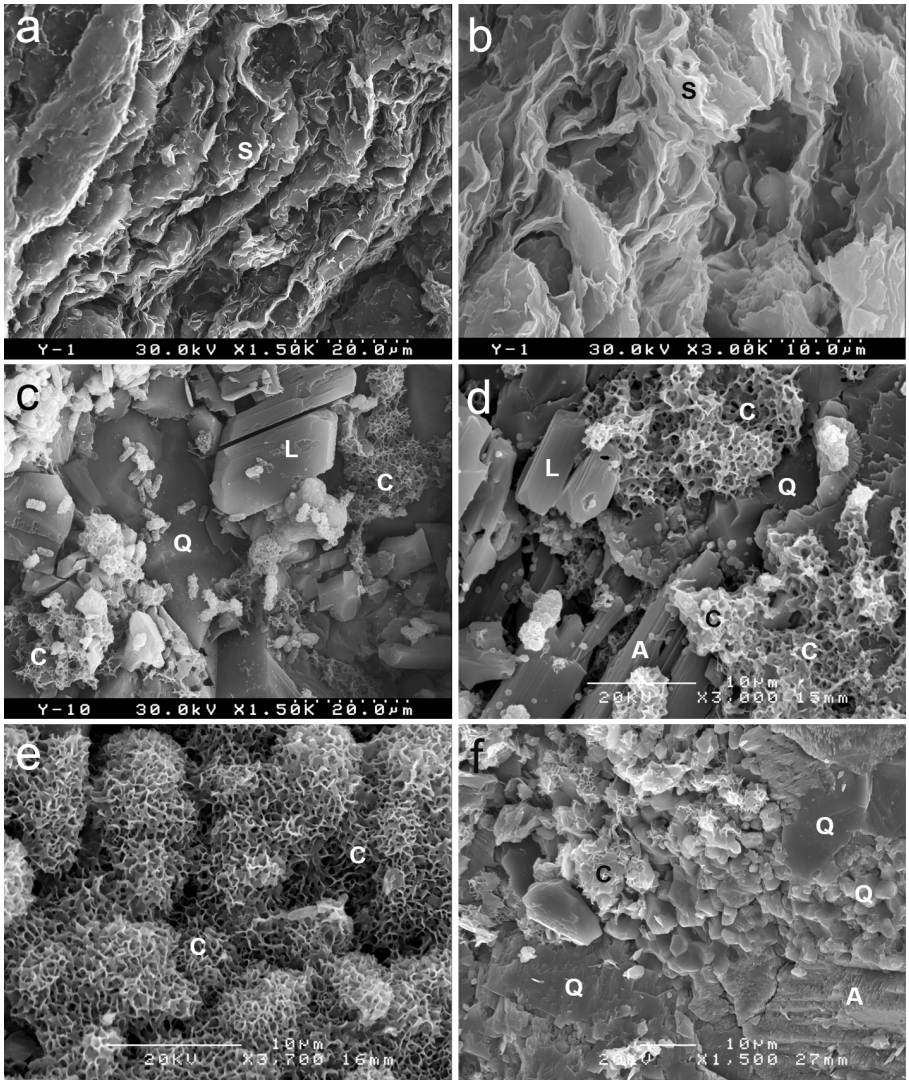

Fig. 5. SEM images of fault materials from the Yukjae Fault. (a) Strong foliation in fault gouge defined by smectite, (b) Residual grains or cavities surrounded by smectite-defined foliation in fault gouge, (c-e) Newly formed laumontite and chlorite in fractured fault rock located 10 cm from fault gouge, (f) Quartz and chlorite in the fractured fault rock located 25 cm from fault gouge. A: albite, C: chlorite, L: laumontite, Q: quartz, S: smectite.

TEM images of fault gouges from the Danguri, Yukjae, Yugye, and Bogyungsa faults show angular to subangular nanometer- to micrometer-sized particles (Fig. 6). These very fine-grained particles do not appear to have undergone severe abrasion, possibly because it is difficult for them to be fractured or abraded to nano-sized ultrafine particles through the size reduction process that occurs during faulting. Clays associated with fractured particles may play an important role in inhibiting abrasion at nanometer scales by acting as a lubricant to assist slip rather than causing friction.

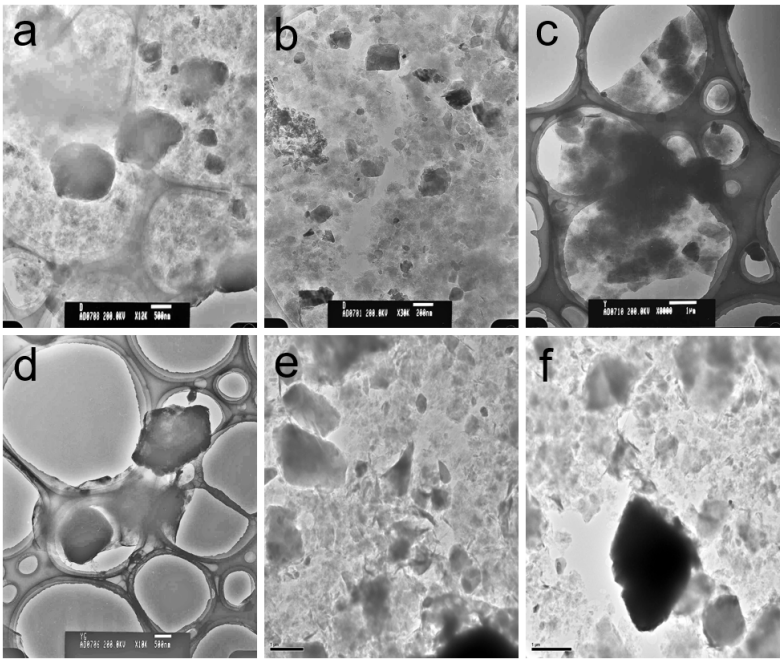

Fig. 6. TEM images of fault gouges showing nanometer to micrometer-sized grains from the (a-b) Danguri, (c) Yukjae, (d) Yugye, and (e-f) Bogyeongsa faults. Scale: 500 nm for (a) and (d), 200 nm for (b), 1 μm for (c), (e), (f).

K-Ar Age Dating on Fault Gouges

Results of K-Ar dating of gouge materials from the studied faults are given in Table 3. The K-Ar ages of the gouges show a wide range from 59.05 to 18.8 Ma. The ages of bulk samples of fault gouges are 47.6 Ma for the Yukjae Fault, 59.1 Ma for the Ansim Fault, 39.4 Ma for the Yugye Fault, and 22.6 Ma for the Bogyeongsa Fault, respectively. These results indicate that the ages of the Yangsan Fault decreases from south to north. The age variation also suggests that the Yangsan Fault did not form during a single event but rather through multiple faulting events over a prolonged period. This conclusion is supported by K-Ar ages of various size fractions in the fault gouges, as presented in Table 3. It is important to note that the age of each fault varies according to the particle-size fraction. with the finer fractions generally having younger ages than the coarser fractions. In particular, the finest fraction of size <0.2 μm yields the youngest age for each fault. This suggests that the finest particles were formed during the most recent faulting events that cumulatively led to the formation of fault gouges. In fractions finer than 2.0 μm, the ages are in the range of 29.8~25.8 Ma for the Danguri Fault, 49.4~40.8 Ma for the Yukjae Fault, 35.4~27.5 Ma for the Ansim Fault, and 20.2~18.8 Ma for the Bogyeongsa Fault, respectively. The age of the Ansim Fault bulk gouge sample is significantly older than those for

the separate fractions: the age of the bulk gouge is 59.1 Ma, whereas it is 35.4 Ma for the 2.0 μm fraction, 31.0 Ma for the 1.0~2.0 μm fraction, 29.3 Ma for the 0.2~1.0 μm fraction, and 27.5 Ma for the finest fraction of size <0.2 μm, respectively. These results suggest that the bulk fraction might contain various K-bearing minerals that originated from detrital host minerals, such as K-feldspars and micas, as well as from authigenic processes. Most the studied fault

Table 3. K-Ar age dating of bulk samples and various size fractions of fault gouges

Size (μm)	K_2O (wt.%)	$^{40}Ar^*$ (10^{-8}ccSTP/g)	Age (Ma)	Host rocks
Danguri <0.2	1.934	195.627	25.871 ± 0.722	Granite, Andesite, Shale, Quaternary sediments
Danguri 0.2~1.0	2.199	232.660	27.052 ± 0.598	
Danguri 1.0~2.0	1.833	205.578	28.663 ± 0.738	
Danguri 2.0	1.745	203.583	29.807 ± 1.017	
Danguri bulk			No data	
Yukjae <0.2	1.314	210.342	40.774 ± 0.935	Sandstone, Mudstone
Yukjae 0.2~1.0	1.183	219.183	47.109 ± 0.977	
Yukjae 1.0~2.0	1.332	258.766	49.364 ± 1.036	
Yukjae 2.0	1.467	273.697	47.433 ± 1.006	
Yukjae bulk	1.167		47.608	
Ansim <0.2	3.159	339.477	27.474 ± 0.558	Red shale, Dark green arkose sandstone
Ansim 0.2~1.0	3.034	347.343	29.254 ± 0.656	
Ansim 1.0~2.0	3.023	367.040	31.010 ± 0.645	
Ansim 2.0	2.495	345.941	35.370 ± 0.747	
Ansim bulk	5.538		59.052	
Yugye bulk	3.836		39.415	Sandstone, Shale
Bogyeongsa <0.2	2.872	210.361	18.771 ± 0.63	Sandstone, Shale, Brecciated lapilli
Bogyeongsa 0.2~1.0	2.885	240.095	21.312 ± 0.601	
Bogyeongsa 1.0~2.0	2.949	232.893	20.231 ± 0.753	
Bogyeongsa 2.0	2.840	222.910	20.107 ± 0.466	
Bogyeongsa bulk	2.699		22.580	

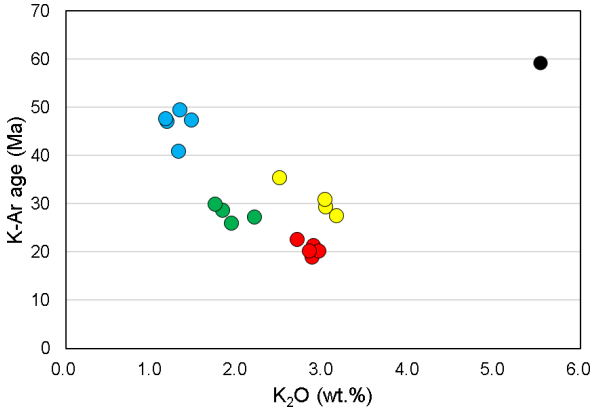

Fig. 7. K-Ar ages vs. K_2O content for fault materials from four sudied faults of the YFS. A black point was from the bulk gouge of the Ansim dam. Green: Danguri, Blue: Yukjae, Yellow: Ansim, Red: Bogyeongsa.

gouges exhibit a general increase in K_2O content with decreasing age (Fig. 7), except for the bulk gouge from the Ansim Fault. This trend reflects an increasing proportions of K-bearing clay minerals, such as illite and interstratified illite/smectite (I/S) phases, in the finer fractions.

Discussion

K-Ar Age in Quaternary Faults and Multiple Faulting

Clay mineral transformations observed in gouges commonly show growth of authigenic $1M_d$ illite, either by transformation of fragmental $2M_1$ illite or muscovite, or growth after the dissolution of K-feldspar (Haines and van der Pluijm, 2012). Fault-gouge dating by application of the IAA method has become an accepted tool for probing fault structural and tectonic histories (Vrolijk et al., 2018). Nevertheless, authigenic illites in fault gouges may consist of various mixtures of illite particles formed at different episode during crystal growth, and therefore, K-Ar ages on illite from fault gouges are often interpreted as maximum ages because the neo-formed illite as the finest separated particle size crystallized at the edges of authigenic clays (Tsukamoto et al., 2020). The K-Ar ages of illite or I/S minerals in fault gouges may be influenced by several factors, including Ar loss, clay diagenesis and the recycling of K of the clay fraction, and dissolution of detrital mica clays by weathering, coupled with and the influx of additional K from outside the fault system (Velde and Renac, 1996; van der Pluijm et al., 2001; Meunier et al., 2004). Although K-Ar dating can still be used to date fault events using illitic clays, age determinations are problematic because multiple faulting events, particle size effect, illite polytype, and illite/smectite (I/S) can greatly affect the determination of real ages. Although only the $1M_d$ type illite polytype in gouge is commonly considered an accurate indicator of the age of a faulting event, different ages on the same fault and particle size effect have always been challenging. Because K-Ar ages obtained from K-bearing secondary minerals including illite and authigenic K-feldspars (Choo and Chang, 2000) in fault gouges are generally mixed, it is difficult to separate only $1M_d$ illite from other K-bearing authigenic minerals. $2M_1$ type illite also forms as Ostwald ripening or rapid precipitation under hydrothermal systems related to faulting. Even though the IAA method has widely been applied, such a method has limitations in determining the ages of the most recent faulting event because Quaternary faulting events along the northern YFS have been not necessarily recorded by K-Ar age dating of fault gouges. For example, it is noteworthy that a Quaternary reverse fault at the Yugye site that was reactivated between 2,400 and 2,000 yr BP is cut by a right-lateral strike-slip fault. Therefore, the latest faulting ages and recurrence intervals for Quaternary active faults of the YFS (e.g., Lee et al., 2015; Song et al., 2020) are considered the most reliable data for evaluating earthquake hazards.

Multiple faulting events have been identified on many faults in the southeastern parts of the Korean Peninsula (Chang and Chang, 1998; Sim et al., 2017; Song et al., 2017, Lee and Kyung, 2022). In this study, multiple faulting events are identified for most faults on the basis of outcrop observations, the presence of veinlets and shearing, and SEM imaging. An analysis of paleostress of the Yangsan Fault (Chang and Chang, 1998) has shown that YSF underwent multiple episodes of deformation involving complex fault movements consisting of strike-slip and dip-slip components during the early Eocene. This complex faulting mechanism may have involved fluid-assisted deformation along the gouge zone.

Formation Condition of Fault Gouges

The fault zones characterized by high porosity and high permeability of fractured fragments facilitate an influx of hydrothermal fluid which subsequently reacts with gouge materials to form clay minerals (e.g., Sibson et al., 1975). Especially, the damage zones around the core zone are characterized by dense fractures and veins. Fracturing and hydrothermal alteration may repeatedly occur with elevated fluid pressure induced by the reduction of pore volume when clay minerals and other secondary minerals form (Chang and Choo, 1998, 1999), which is suggested by a seismic pump theory (Sibson et al., 1975). The occurrence of smectite, laumontite, and calcite in fault gouges and fractured fault rocks indicates low grade hydrothermal alteration under high water-rock ratio conditions associated with earthquake events, accompanying filling fissures. In this study, clay minerals from fault materials in the northern YFS consist of smectite, chlorite, kaolinite, zeolites, and illite. Illite occurs mostly as $1M_d$ with lesser $2M_1$ polytype. Chlorite is also an important product of hydrothermal alteration within fault zones (Belzer and French, 2022). The mineralogical features of abundant smectite and lM_d type with lesser quantities of zeolites indicate that fault gouges were derived from hydrothermal alteration at low temperatures right after faulting. Zeolites, including laumontite and mordenite, have been found in various fault rocks in the eastern Korean Peninsula (Choo and Chang, 2000; Choo et al., 2012; Moon et al., 2015; this study), which suggests low temperature conditions of 100~200°C (Chang and Choo, 1999 and references therein) characterized by the generation of calcic plagioclase as a degradation product.

Slip Behavior of Faults Related to Clay Minerals

Formation of hydrous minerals such as clay minerals and zeolites can accelerate fault reactivation (Sibson, 1977). The slip behavior of faults has been highly dependent on mineralogical and fluid processes in fault gouges because the composition of gouge significantly affects the frictional strength of the fault. Clay minerals as well as the filling of veins of calcite and zeolites can affect the frictional properties a large fault. Different clay types in fault cores have varying friction coefficients, affecting the sliding or reactivation of faults. The presence of phyllosilicates in fault gouge have important implications for weakening the frictional strength of faults (Collettini et al., 2009; Tembe et al., 2010; Haines and van der Pluijm, 2012; Sakuma et al., 2022). For example, the friction coefficient of montmorillonite is lower than that of illite shale under the same conditions, meaning that a fault would more easily slide on gouge containing the former than the latter clay type (Saffer and Marone, 2003; Cai et al., 2022).

The composition and structure of fault gouges are the key factors that affect the different magnitudes and frequencies of seismic activity (Cai et al., 2022). In five Quaternary faults, smectite is always abundant even in finer fractions. Chlorite-rich fault rocks play an important role in controlling megathrust fault slip (Okamotoa et al., 2019, 2020). The fault gouge from the fault core at Bogyeongsa exhibits a low peak friction coefficient of 0.2 as a result of the high content of montmorillonite (Woo et al., 2015), and the fault there would be expected to slip more readilt than other faults of the YFS. The role of authigenic clay growth in fault gouges has been increasingly important for understanding the mechanics of brittle faulting and fault zone processes, including creep, seismogenesis and the frictional strength of brittle faults (Haines and van der Pluijm, 2012). Especially, properties of clay minerals associated with fluids play an important role in shallow faults (Evans and Chester, 1995; Vrolijk and van der Pluijm, 1999; Schleicher et al., 2009).

Fault gouges are generally considered to form during seismic faulting related to high-magnitude earthquakes; for example, M7.5 in the Tianjingshan-Xiangshan fault in China (Zhang et al., 2002) and M7.2 in Kobe (Enomoto and Zheng, 1998). Estimates of the maximum earthquake magnitude along the Yangsan Fault are as follows: M6.7~7.0 at a trench site of the Danguri Fault (Song et al., 2020), M6.5~7.5 (Kim and Jin, 2006) and M6.8 (Kyung, 2010) for the Yugye Fault, and M6.0~6.7 for the Bogyeongsa Fault (Lee et al., 2022).

Quaternary faulting events along the northern Yangsan Fault should be treated as more decisive information on multiple faulting, irrespective of K-Ar age dating on fault gouges. Therefore, in addition to age determinations of faulting, it is important to consider the types and amounts of clay minerals in fault gouges in order to understand faulting histories and the reactivation of seismic faults.

Conclusions

Fluid-assisted processes also play a part in the evolution of gouge zones during the periods between faulting events. In fractions below 2.0 μm, K-Ar ages are in the range of 29.8~25.8 Ma in the Danguri Fault, 49.4~40.8 Ma in the Yukjae Fault, 35.4~27.5 Ma in the Ansim Fault, and 20.2~18.8 Ma in the Bogyeongsa Fault, respectively. Because fault gouges in the five Quaternary faults studied consist of smectite and chlorite, with lesser amounts of illite, zeolite, and kaolinite, hydrothermal alteration of the gouges is considered to have occurred in a low temperature (100~200°C) environments right after faulting. The presence of a clay-defined foliation and veinlets, together with a wide range of K-Ar age data, indicate multiple faulting events at the studied sites along the northern YFS. In addition to K-Ar age dating of faulting, it is important to consider the microstructural features and amounts of of clay minerals in fault gouges when trying to understand the movement history and possible reactivation of of seismic faults.

Acknowledgments

This study was performed with the support of the R&D Program for Forest Science Technology (Project No. FTIS 2021348A00-2123-CD01) provided by Korea Forest Service (Korea Forestry Promotion Institute).

References

Belzer, B.D., French, M.E., 2022, Frictional constitutive behavior of chlorite at low shearing rates and hydrothermal conditions, Tectonophysics, 837, 229435.

Cai, Z., Huang, Q., Huang, Q., Lu, L., Huang, X., 2022, The composition and structure of fault gouge affect the magnitude and frequency of seismic activity in the Red River Fault Zone, Arabian Journal of Geosciences, 15, 663.

Chang, C.J., 2001, Structural characteristics and evolution of the Yangsan fault, SE Korea, Ph.D. Thesis, Kyungpook National University, 259p (in Korean with English abstract).

Chang, C.J., Chang, T.W., 1998, Movement history of the Yangsan Fault based on paleostress analysis, Journal of Engineering Geology, 8(4), 36-49 (in Korean with English abstract).

Chang, T.W., Choo, C.O., 1998, Formation processes of fault gouges and their K-Ar ages along the Dongae fault, The

Journal of Engineering Geology, 8(2), 175-188 (in Korean with English abstract).

Chang, T.W., Choo, C.O., 1999, Faulting processes and K-Ar ages of fault gouges in the Yangsan fault zone, Journal of Korean Earth Science Society, 20(1), 25-37 (in Korean with English abstract).

Choo, C.O., Chang, T.W., 2000, Characteristics of clay minerals in gouges of the Dongrae fault, southeastern Korea, and implications for fault activity, Clays and Clay Minerals, 48(2), 204-212.

Choo, C.O., Jang, Y.D., Chang, C.J., 2012, Mineralogical characteristics of hydrothermal laumontite and adularia in the breccia zone of a fault, Yangbuk-myeon, Gyeongju and implications for fault activity, Journal of Mineralogical Society of Korea, 25(1), 23-36 (in Korean with English abstract).

Choo, C.O., Jo, S.H., Lee, S.Y., Lee, S.E., Jeong, G.C., 2020, Characterization of pseudotachylite and fault gouges in drill cores from Andong, Korea and its implications for paleo-earthquakes, Sustainability, 12, 10421.

Collettini, C., Niemeijer, A., Viti, C., Marone, C., 2009, Fault zone fabric and fault weakness, Nature, 462, 907-910.

Enomoto, Y., Zheng, Z., 1998, Possible evidences of earthquake lightning accompanying the 1995 Kobe earthquake inferred from the Nojima fault gouge, Geophysics and Geophysical Letters, 25(14), 2721-2724.

Evans, J.P., Chester, F.M., 1995, Fluid-rock interaction in faults of the San Andreas system: Inferences from San Gabriel fault rock geochemistry and microstructures, Journal of Geophysical Research, 100, B7, 13007-13030.

Haines, S.H., van der Pluijm, B.A., 2012, Patterns of mineral transformations in clay gouge, with examples from low-angle normal fault rocks in the western USA, Journal of Structural Geology, 43, (1) 2-32.

Kim, Y.S., Jin, K., 2006, Estimated earthquake magnitude from the Yugye Fault displacement on a trench section in Pohang, SE Korea, Journal of the Geological Society of Korea, 42(1), 79-94 (in Korean with English abstract).

Kyung, J.B., 2010, Paleoseismological study and evaluation of maximum earthquake magnitude along the Yangsan fault and Ulsan fault zones in the southeastern park of Korea, Geophysics and Geophysical Exploration, 13(3), 187-197.

Lee, J., Rezaei, S., Hong, Y., Choi, J.H., Choi, J.H., Choi, W.H., Rhee, K.W., Kim, Y.S., 2015, Quaternary fault analysis through a trench investigation on the northern extension of the Yangsan fault at Dangu-ri, Gyungju-si, Gyeongsang-buk-do, Journal of the Geological Society of Korea, 51(5), 471-485 (in Korean with English abstract).

Lee, K., Kyung, J.B., 2022, Active faults of the southern Korean peninsula, Journal of National Academy Sciences of Korea, 61(1), 83-117 (in Korean with English abstract).

Lee, S., Han, J., Ha, S., Lim, H., Seong, Y.B., Choi, J.H., Lee, C.H., Kim, S.J., Kang, H.C., Kim, M.C., Lim, H., Son, M., 2022, Characteristics of the Quaternary faulting detected along the Yangsan Fault in Yugye- and Jungsan-ri, northern Pohang city, Journal of Geological Society of Korea, 58(4), 427-443 (in Korean with English abstract).

Meunier, A., Velde, B., Zalba, P., 2004, Illite K-Ar dating and crystal growth processes in diagenetic environments: A critical review, Terra Nova, 16, 296-304.

Moon, S.W., Yun, H.S., Choo, C.O., Kim, W.S., Seo, Y.S., 2015, A study on mineralogical and basic mechanical properties of fault gouges in 16 faults, Korea, Journal of the Mineralogical Society of Korea, 28(2), 109-126 (in Korean with English abstract).

Okamoto, A.S., Verberne, B.A., Niemeijer, A.R., Takahashi, M., Shimizu, I., Ueda, T., Spiers, C.J., 2019, Frictional properties of simulated chlorite gouge at hydrothermal conditions: Implications for subduction megathrusts, Journal of Geophysical Research: Solid Earth, 124, 4545-4565.

Okamotoa, A., Niemeijer, A.R., Takeshitaa, T., Verbernec, B.A., Spiers, C.J., 2020, Frictional properties of actinolite-chlorite gouge at hydrothermal conditions, Tectonophysics, 779, 228377.

Pevear, D.R., 1992, Illite age analysis, a new tool for basin thermal history analysis, In: Kharaka, Y.K., Maest, A.S. (eds.), Water-Rock Interaction, Balkema, A.A., Rotterdam, 1251-1254.

Pevear, D.R., 1999, Illite and hydrocarbon exploration, Proceedings of the National Academy of Sciences, 96, 3440-3446.

Saffer, D.M., Marone, C., 2003, Comparison of smectite- and illite-rich gouge frictional properties: application to the updip

limit of the seismogenic zone along subduction megathrusts, Earth and Planetary Science Letters, 215, 219-235.

Sakuma, H., Lockner, D.A., Solum, J., Davatzes, N.C., 2022, Friction in clay-bearing faults increases with the ionic radius of interlayer cations, Communications Earth & Environment, 3, 116-123.

Schleicher, A.M., Tourscher, S., van der Pluijm, B.A., Warr, L.N., 2009, Constraints on mineralization, fluid-rock interaction and mass transfer during faulting at 2-3 km depth from the SAFOD drill hole, Journal of Geophysical Research, 114, B04202.

Sibson, R.H., 1977, Fault rocks and fault mechanisms, Journal of Geological Society of London, 133, 1910213.

Sibson, R.H., Moore, J.M.M., Rankin, A.H., 1975, Seismic pumping - a hydrothermal fluid transport mechanism, Journal of the Geological Society, 131, 653-659.

Sim, H., Song, Y., Son, M., Park, C., Choi, W., Khulganakhuu, C., 2017, Reactivated timings of Yangsan fault in the northern Pohang area, Korea, Economic and Environmental Geology, 50(2), 97-104 (in Korean with English abstract).

Solum, J.G., Hickman, S.H., Lockner, D.A., Moore, D.E., van der Pluijm, B.A., Schleicher, A.M., Evans, J.P., 2006, Mineralogical characterization of protolith and fault rocks from the SAFOD Main Hole, Geophysical Research Letters, 33, L21314.

Song, S,J., Choo, C.O., Chang, C.J., Jang, Y.D., 2017, A microstructural study of the fault gouge in the granite, Yangbuk, Gyeongju, southeastern Korea, with implications for multiple faulting, Geosciences Journal, 21, 1-19.

Song, Y., Ha, S., Lee, S., Kang, H.C., Choi, J.H., Son, M., 2020, Quaternary structural characteristics and paleoseismic interpretation of the Yangsan Fault at Dangu-ri, Gyeongju-si, SE Korea, through trench survey, Journal of the Geological Society of Korea, 56(2), 155-173 (in Korean with English abstract).

Song, Y., Sim, H., Hong, S., Son, M., 2019, K-Ar Age-dating results of some major faults in the Gyeongsang basin: Spatio-temporal variability of fault activations during the Cenozoic Era, Econmic and Environmental Geology, 52(5), 449-457 (in Korean with English abstract).

Tembe, S., Lockner, D.A., Wong, T.F., 2010, Effect of clay content and mineralogy on frictional sliding behavior of simulated gouges: Binary and ternary mixtures of quartz, illite, and montmorillonite, Journal of Geophysical Research, 115, B03416.

Tettenhorst, R.T., Corbató, C.E., 1993, Quantitative analysis of mixtures of 1M And $2M_1$ dioctahedral micas by X-Ray diffraction, Clays and Clay Minerals, 41, 45-55.

Tsukamoto, S., Tagami, T., Zwingmann, H., 2020, Direct dating of fault movement, In: Tanner, D., Brandes, C. (eds.), Understanding Faults - Detecting, Dating, and Modeling, Elsevier, 257-282.

van der Pluijm, B.A., Hall, C.M., Vrolijk, P.J., Pevear, D.R., Covey, M.C., 2001, The dating of shallow faults in the Earth's crust, Nature, 412, 172-175.

Velde, B., Renac, C., 1996, Smectite to illite conversion and K-Ar ages, Clay Minerals, 31, 25-32.

Vrolijk, P., Pevear, D., Covey, M., LaRiviere, A., 2018, Fault gouge dating: History and evolution, Clay Minerals, 53, 305-324.

Vrolijk, P., van der Pluijm, B.A., 1999, Clay gouge, Journal of Structural Geology, 21, 1039-1048.

Woo, S., Lee, H., Han, R., Chon, C.M., Son, M., Song, I., 2015, Frictional properties of gouges collected from the Yangsan Fault, SE Korea, Journal of the Geological Society of Korea, 51(6), 569-584 (in Korean with English abstract).

Zhang, B., Lin, C, Shi, L., 2002, Microstructural features of fault gouges from Tianjingshan-Xiangshan fault zone and their geological implications, Science in China (Series D) 45(1), 72-80.